

# Lecture Notes Particle Astrophysics

## Neutrinos

Spring 2003

dr. H. J. Bulten  
email: [henkjan@nikhef.nl](mailto:henkjan@nikhef.nl)

Department of Physics and Astronomy, Vrije Universiteit  
Amsterdam, The Netherlands

links to some additional information will be available at the web: <http://www.nikhef.nl/~henkjan>

# Contents

|          |  |          |
|----------|--|----------|
| <b>1</b> | <b>Solar Neutrino Problem</b>                  | <b>3</b> |
| 1.1      | Introduction . . . . .                         | 3        |
| 1.2      | Solar models . . . . .                         | 3        |
| 1.3      | Solar Neutrino Detection . . . . .             | 8        |
| 1.4      | Neutrino oscillations . . . . .                | 11       |
| 1.4.1    | Matter Oscillations . . . . .                  | 13       |
| 1.5      | Second generation neutrino detectors . . . . . | 15       |
| 1.6      | Neutrino parameters. . . . .                   | 17       |

# 1 Solar Neutrino Problem

## 1.1 Introduction

In astrophysics, detailed models have been developed to obtain a description of stars. These models have been successful in predicting and explaining a wide variety of observations (e.g. the distribution of stars along the Hertzsprung-Russell diagram) and have been honed to high precision nowadays. According to all present solar models, the sun produces almost all of its energy by fusion, mainly by protons are converted into  ${}^4\text{He}$  and  ${}^8\text{Be}$  nuclei (the p-p chain). It is obvious that in this process electrons and neutrinos are produced. Although the solar model makes accurate predictions for a number of observables, the predicted neutrino rates are about a factor of two to three higher than the observed rates in the present generation of neutrino-detection experiments. This discrepancy indicates that either the current solar models are wrong, or that new physics occurs in the neutrino sector of the standard model (neutrino decay, neutrino oscillations), implying that neutrinos do have mass. In this chapter, we will scrutinize the evidence for the solar neutrino problem and discuss a strong candidate for explaining the discrepancy, namely neutrino oscillations. In subsection 1.2, a state-of-the-art solar model is discussed. In subsection 1.3, the current and proposed solar neutrino detection experiments are reviewed. In section 1.4, the formalism of neutrino oscillations is given. In section 1.5, some new large neutrino detectors are discussed. In the last section, the current status on limits on the neutrino mass and on oscillation parameters is reviewed. For further reading I suggest the book *Neutrino Astrophysics* by Bahcall, Cambridge University Press (1989), as well as the web sites that can be found from my home page.

## 1.2 Solar models

In the last four decades a lot of effort has been put into refining solar models. In this field of astrophysics, it is customary to refer to the most up-to-date model that includes the latest data on e.g. the age or luminosity of the sun as the "standard model". Since this model is continuously refined, we will use results from the model of Bahcall *et al.* [1, 2, 3] as an example for solar models.

In order to calculate the properties of the sun, the model needs input data. The model starts with an amount of gas with hydrogen,  ${}^4\text{He}$ , and metal isotopes (in astrophysics every nucleus with  $Z > 2$  is referred to as metal) with the right mass. The current radius, luminosity, isotopic abundances, surface temperature etc. is then calculated by evolving the equations of state of the sun in steps of typically 500 million years to the current age.

Neutrinos from the sun stem mainly from two sources. The sun burns hydrogen to heavier masses in the p-p chain (see table I), and in the core of the sun neutrinos are produced in the C-N-O cycle, for which the three most important processes are

$${}^{13}\text{N} \rightarrow {}^{13}\text{C} + e^+ + \nu_e \quad (q_\nu \leq 1.199\text{MeV}),$$

$${}^{15}\text{O} \rightarrow {}^{15}\text{N} + e^+ + \nu_e \quad (q_\nu \leq 1.732\text{MeV}),$$

and

$${}^{17}\text{F} \rightarrow {}^{17}\text{O} + e^+ + \nu_e \quad (q_\nu \leq 1.740\text{MeV}),$$

with  $q_\nu$  the energy of the produced electron neutrino. Table 1 gives the most important reactions in the so-called p-p chain, from which most neutrinos originate. For these

reactions the Q-value, i.e. the nuclear energy released in the reaction, is given, as well as the average energy of the neutrino. The lifetime is the average time that the parent nucleus can exist before it is converted by the specified reaction.

Table 1: The total nuclear-energy release, average neutrino energy, and lifetimes for the most important reactions in the p-p chain

| reaction   | Q [MeV] | $\langle q_{\nu_e} \rangle$ | Lifetime [yr] |
|--|---------|-----------------------------|---------------|
| ${}^1H(p, e^+\nu_e){}^2H$ (pp)                           | 1.442   | 0.265                       | $10^{10}$     |
| ${}^1H(pe^-, \nu_e){}^2H$ (pep)                          | 1.442   | 1.442                       | $10^{12}$     |
| ${}^2H(p, \gamma){}^3He$                                 | 5.494   | -                           | $10^{-8}$     |
| ${}^3He(p, e^+\nu_e){}^4He$                              | 19.795  | 9.625                       | $10^{12}$     |
| ${}^3He({}^3He, 2p){}^4He$                               | 12.860  | -                           | $10^5$        |
| ${}^3He({}^4He, \gamma){}^7Be$                           | 1.586   | -                           | $10^6$        |
| ${}^7Be(e^-, \nu_e){}^7Li$                               | 0.862   | 0.862                       | $10^{-1}$     |
| ${}^7Li(p, \alpha){}^4He$                                | 17.347  | -                           | $10^{-5}$     |
| ${}^7Be(p, \gamma){}^8B$                                 | 0.137   | -                           | $10^2$        |
| $({}^8B, e^+\nu_e){}^8Be^*$ ; $({}^8Be^*, \alpha){}^4He$ | 17.98   | 6.71                        | $10^{-8}$     |

The majority of the neutrinos originate from the pp reaction. However, these neutrinos have a small kinetic energy and are hard to detect. The most important source for high-energy neutrinos in the sun is  ${}^8B$ . Fig. 1.2 gives the energy spectrum of the solar neutrinos as deduced in the model of Bahcall [2].

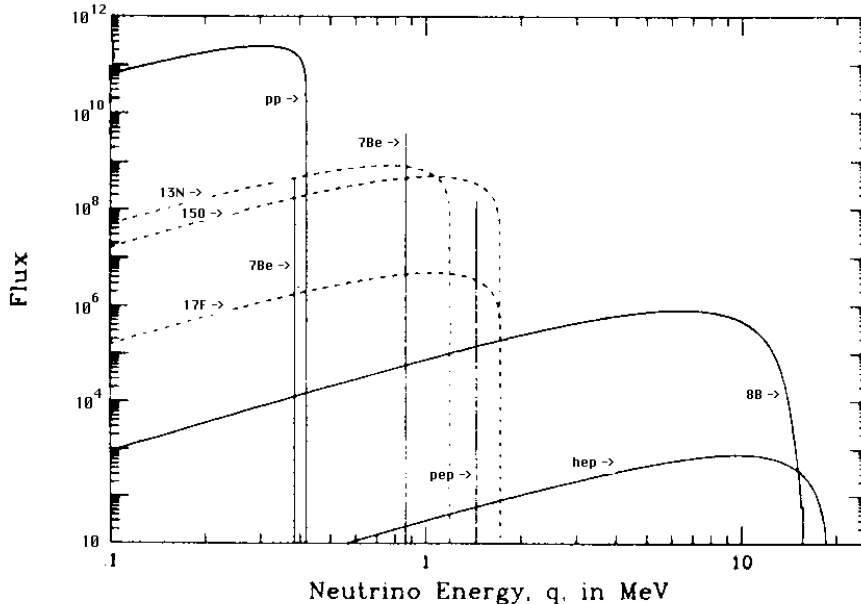


Figure 1: Energy spectrum for solar neutrinos.

We are especially interested in the precision in which the neutrino flux can be calculated. These rates obviously depend on the parameters of the model. Bahcall *et al.* [1] estimated the uncertainties in the neutrino fluxes by studying the dependences on all model parameters. These parameters are:

- Nuclear reaction rates.

The calculations are quite accurate, small effects like vacuum polarization have been included. Uncertainties in the resulting neutrino production rates are less than 1 % for the total number of neutrinos. However, the low-energy  $p\text{-}^7\text{Be}$  reaction rate is known with less precision, leading to about 15 % uncertainty in the number of  $^8\text{B}$  neutrinos.

- Solar luminosity.

The solar luminosity fluctuates with the well-known 11 year solar cycle. Further sources of uncertainty in the absolute solar luminosity is given by a) the absolute calibration of satellite radiometers and b) long-term fluctuations in the solar luminosity. The applied solar luminosity equals  $L = 1367 (5) \text{ W/m}^2$  at one A.U. distance from the sun. The resulting uncertainty in neutrino rate equals 3 %.

- Solar age.

The solar age has been obtained from measurements of isotopes in meteorites. Some objects have been formed in the presolar nebula, others after "ignition" of the sun (for a discussion see [1]). The current consensus is an age of  $4.57 (2) \times 10^9$  years. The resulting uncertainty in the neutrino rate amounts to less than 1 %.

- Primordial element abundances and diffusion.

The density of metals in the sun influence strongly the radiative opacity, and hence the temperature gradient. As an estimate, one may use the spread in the results of different solar models. Ref. [1] estimates the uncertainty on the abundance of metals to be about 6 %. One uncertainty in the determination of the primordial abundances is due to the effect of diffusion: due to gravity the heavier nuclei tend to drift towards the core of the sun. Note, that this is a slow process; typically it takes  $10^{13}$  years to diffuse a solar radius under solar conditions. Since this diffusion occurs, it is somewhat difficult to relate measured abundances from spectroscopy to primordial element abundances. Diffusion both affect helioseismologic predictions and the neutrino fluxes; the resulting uncertainty in the flux of pp neutrinos (the first reaction in table 1) is about 0.6 %; the uncertainty in neutrinos from the CNO cycle about 12 %.

- Radiative opacities.

Most energy in the sun is released in the form of photons. The thermal gradient strongly depends on the opacity. Although the uncertainty in opacity influences helioseismologic data, the influence on the neutrino rates appears to be small.

- Neutrino interaction cross section.

The neutrino interaction cross section only very slightly influences the spectrum from the sun (rescattering effects); on the other hand it directly influences the predicted *detected* neutrino rates in the experiments. The uncertainties therefore depend on the detection technique. These uncertainties are included in the result of Table 1.2. Also, the contribution of each reaction chain to Gallium and Chlorine detectors is given in this table in standard neutrino units ( 1 SNU equals  $10^{-36}$  interaction per second per atom of target material at 1 astronomical unit distance from the center of the sun).

The solar model can be tested by determining the neutrino spectrum. Fig. 1.2 demonstrates, that the the neutrinos from the most important reaction chains are produced in different regions of the sun (due to the dependence of the reaction rates on temperature). If the solar model has a flaw, it will show up in a different distribution of neutrinos from these sources. E.g. the production rate of  $^8\text{B}$  depends on the temperature of the sun in the center  $T_c$  with about  $T_c^{18}$ , whereas the other reaction chains are much less sensitive to  $T_c$ . A lower central temperature should show up as a depletion of  $^8\text{B}$  neutrinos. How-

Table 2: Neutrino rates from the most important sources and their uncertainties.

| source          | Flux<br>$10^8 \text{ cm}^{-2} \text{ s}^{-1}$ | uncertainty<br>% | Gallium rate<br>SNU | Chlorine rate<br>SNU |
|-----------------|---|------------------|---------------------|----------------------|
| pp              | 591   | $\pm 1$          | 70                  | 0                    |
| pep             | 1.40  | +1 / -2          | 3.0                 | 0.22                 |
| $^7\text{Be}$   | 51.5  | +6/-7            | 38                  | 1.2                  |
| $^8\text{B}$    | $6.62 \times 10^{-2}$                         | +14 / -17        | 16                  | 7.4                  |
| $^{13}\text{N}$ | 6.18  | +17/-20          | 3.8                 | 0.11                 |
| $^{15}\text{O}$ | 5.45  | +19/-22          | 6.3                 | 0.37                 |
| $^{17}\text{F}$ | $6.48 \times 10^{-2}$                         | +15/-19          |                     |                      |
| total           |   |                  | $137^{+8}_{-7}$     | $9.3^{+1.2}_{-1.4}$  |

ever, only the magnitude of the neutrino spectrum for a certain target can change; the spectrum above 2 MeV should follow the Boron spectrum closely.

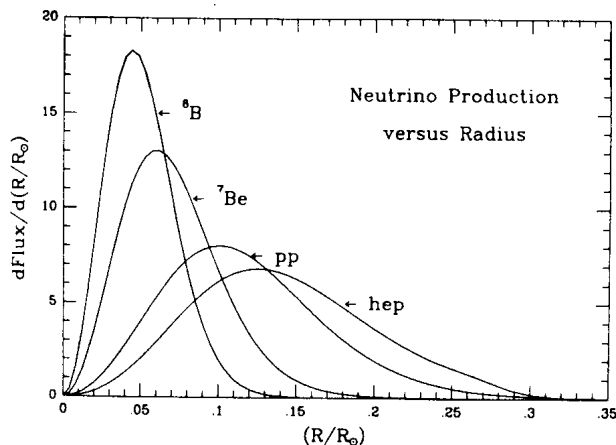


Figure 2: Neutrino production as a function of the distance to the center of the sun.

Apart from measuring the energy spectrum of the solar neutrinos, one can test the solar model in an independent way by comparing its predictions to helioseismologic data. Helioseismology provides information on the structure of the sun in a similar way as terrestrial seismology, by analyzing the very slight motions of the surface of the sun. Leighton, Noles, and Simon [4] first observed solar oscillations by studying velocity shifts in the spectral absorption lines formed in the surface area of the sun. They found that the surface of the sun is filled with patches that oscillate with periods of about 5 minutes and velocity amplitudes of about 0.5 km/s. One such a patch typically covers an area with a diameter of a few percent of the solar diameter.

Sound waves that are excited in the core of the sun are largely trapped between the surface and a region that is close to the base of the convective zone (at about 0.713 solar diameters). The sun acts as a resonant cavity for these waves. The observed motions at the surface is due to the interference of millions of these sound waves. In this model, the frequencies of the surface oscillations are asymptotically described by [2]

$$\nu_{n,l} = \nu_0 \left\{ n + \frac{l}{2} + \epsilon - \frac{\alpha l(l+1) - \beta}{n + \frac{l}{2} + \epsilon} \right\} \quad (1)$$

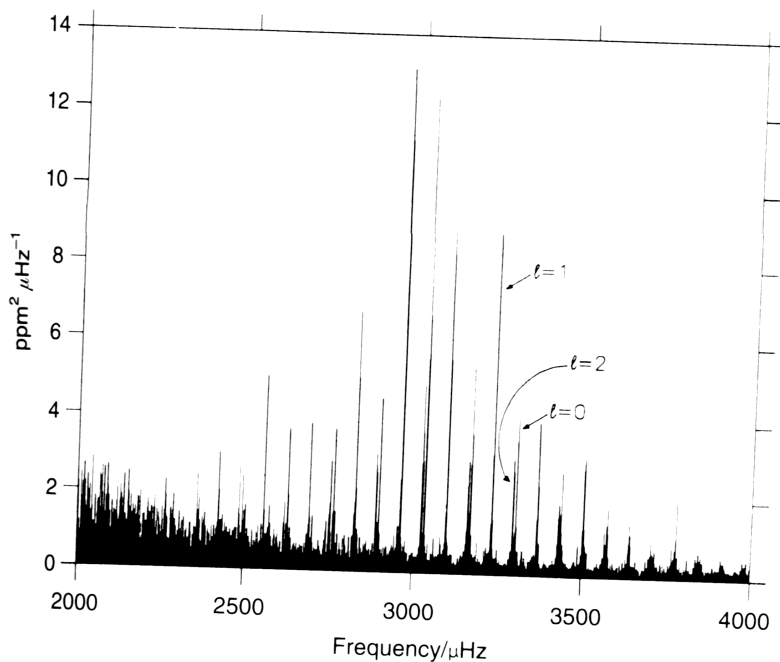


Figure 3: An example of the frequency spectrum of solar oscillations, showing some of the normal modes of the sun. This spectrum of low-degree p-mode oscillations shows alternating double peaks ( $l = 0, 2$ ) and single peaks ( $l = 1$ ).

with  $\nu_{n,l}$  the frequency of the  $n^{\text{th}}$  eigenmode that is described by the spherical harmonic  $Y_m^l(\theta, \phi)$ . A spectrum of frequencies can be observed. As an example the magnitude of variation of surface temperature is plotted as a function of the frequency for low degree p-modes in Fig. 1.2. The data were obtained during a 160 period with the IPHIR experiment on board of the PHOBOS satellite [6]. From these observations one can compare the sound speed in the sun as a function of the radial distance (see Fig. 1.2), which is closely related to the opacity. The observations are described with a precision of typically better than 0.2 % by present solar models [1, 5], when the effect of metal diffusion is included.

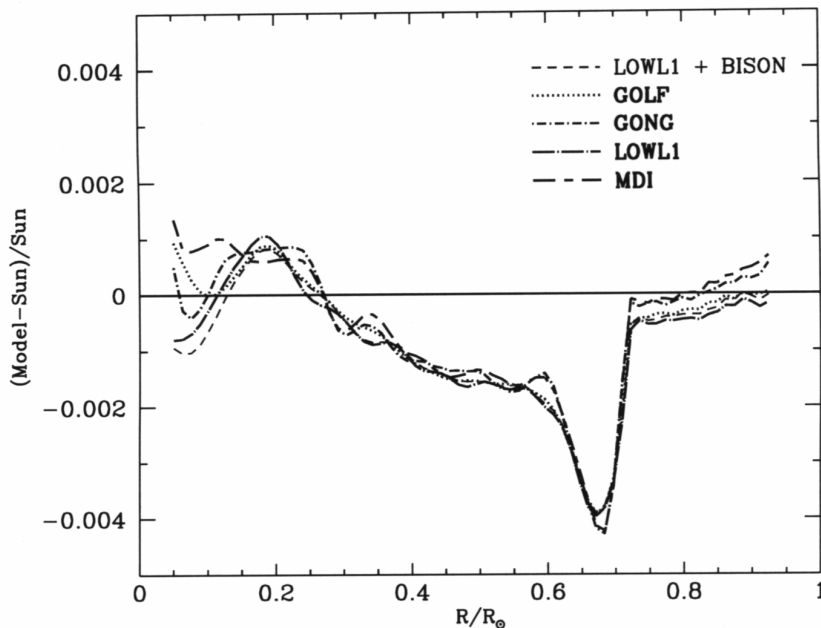


Figure 4: The ratio of the calculated speed of sound for the standard model of Bahcall and the observed speed of sound in the sun for five recent experiments as a function of the radial distance to the center of the sun (see [5] and refs. therein).

### 1.3 Solar Neutrino Detection

Neutrino detection is tedious, because of the small Fermi coupling constant of the weak interaction. Note, that the cross sections for neutrino detection in matter are typically more than 30 orders of magnitude smaller than electron or muon cross sections. Some cross sections are given in the table below.

Therefore large detectors are needed to obtain enough events. In addition, good shielding from background events is necessary. (Even at 4000 meters below sea level, high-energy cosmic muons give typically  $10^6$  times more often a trigger in a Cerenkov detector than neutrinos, which are much more abundant). It comes as no surprise, that even nowadays the fluxes of neutrinos from the sun are only known to the 10 % level.

The first large-scale neutrino detector that was constructed was the detector of the **Homestake** experiment, named after the South Dakota gold mine in which the detector was placed [7]. The detector contained perchloroethylene ( $C_2Cl_4$ ), which is liquid at room temperature. The reaction  $^{37}Cl(\nu_e, e^-)^{37}Ar$  with a threshold of 814 keV is applied to determine the flux of solar neutrinos above that energy. The experiment is sensitive to all neutrino sources in the sun, with the exception of the dominant pp neutrinos. The detector contained  $2.2 \times 10^{30}$  Chlorine atoms. The produced  $^{37}Ar$  atoms were extracted typically every 60 days. The  $^{37}Ar$  atoms could be identified by their radioactive decay to  $^{37}Cl$ , which dominantly proceeds via K-shell electron capture. The  $^{37}Cl$  atom is thus produced with a hole in the K-shell. This hole is quickly filled with the emittance of either a 2.82 keV Auger electron (the dominant process) or a Röntgen photon. More than 80 % of the  $^{37}Ar$  atoms will decay to  $^{37}Cl$  under the emittance of this 2.82 keV Auger electron. This electron will give a fast-rising monoenergetic signal in the detectors that are applied to analyze the gas. The unique signature of the signal provides the means to separate

Table 3: Neutrino cross sections in  $10^{-50}m^2$  on different materials. The cross section on the electron is a scattering cross section, the other cross sections are nuclear absorption cross sections.

| $E_\nu$ | $\sigma$ on $e^-$ | $\sigma$ on $^2\text{H}$ | $\sigma$ on $^{37}\text{Cl}$ | $\sigma$ on $^{71}\text{Ga}$ |
|---------|-------------------|--------------------------|------------------------------|------------------------------|
| 0.2     |                   | 0                        | 0                            | 0                            |
| 0.4     |                   | 0                        | 0                            | 24.6                         |
| 1       | 71                | 0                        | 5.2                          | 101                          |
| 2       | 163               | 33                       | 37                           | 406                          |
| 5       | 445               | 3240                     | 563                          | 4480                         |
| 10      | 919               | $2.59 \times 10^4$       | $2.77 \times 10^4$           | $5.84 \times 10^4$           |

signals from the decay of  $^{37}\text{Ar}$  from background in the detector (predominantly due to cosmic radiation).

Assuming 100 % extraction efficiency the amount of extracted argon atoms equals

$$N_{ext} = \sum_i \{ \Phi_i \sigma_i + BCKGR \} N_0 T_0 (1 - e^{-t/T_0})$$

with  $\Phi_i$  the flux of a neutrino species through the detector,  $\sigma_i$  the cross section of the reaction for this species (which depends on the energy spectrum),  $BCKGR$  the amount of interactions caused by background processes,  $N_0$  the amount of  $^{37}\text{Cl}$  atoms in the detector,  $T_0$  the life time of the radioactive Argon atoms (50.5 days) and  $t$  the integrated time between extractions.

The most important contribution to unwanted background events stems from cosmic radiation. A few high-energetic muons penetrate to the depth of the Homestake detector and produce protons in the detector with enough kinetic energy to induce the reaction  $^{37}\text{Cl}(p,n)^{37}\text{Ar}$ . Also the natural radioactivity of the earth will lead to a few background events. Therefore all solar neutrino detection experiments take place well below the surface of the earth, and usually precautions are taken like the use of radiation-low materials (such as application of lead that came from sunken galleons).

The extraction efficiency of  $^{37}\text{Ar}$  atoms is monitored by injecting a small quantity of tracer gas,  $^{36}\text{Ar}$  or  $^{38}\text{Ar}$ . The extraction efficiency proved to be stable and around 95 % over the 25 years that the Homestake experiment was in operation. A few hundred  $^{37}\text{Ar}$  atoms were extracted from the  $1.3 \times 10^5$  kg of chlorine atoms between 1970 and 1995, yielding  $\sum \Phi_i \sigma_i = 2.55 \pm 0.17(stat) \pm 0.18(syst)$ , where the systematic error is dominated by the uncertainty in the amount of background events.

Two other radiochemical experiments, **Gallex** [8, 9] in Italy and **SAGE** [13] in the Caucasus applied Gallium. Since the reaction  $^{71}\text{Ga}(\nu_e, e^-)^{71}\text{Ge}$  has a threshold of only 233 keV, these two experiments are sensitive to the dominant p-p neutrinos as well. The SAGE experiment initially employed 30 tons, and later 57 tons of Gallium, which is stored in 8 chemical reactors. The extraction of germanium is based on the fact that the melting point of gallium is 29.8 °C, hence it can be kept in liquid form. The Germanium is extracted and distilled typically once a month by a procedure that is detailed in Ref. [13]. In order to determine the efficiency of the extraction procedure about 700  $\mu\text{gr}$  of natural Ge is added, equally distributed over the 8 tanks. The extraction efficiency is typically around 80 %.

$^{71}\text{Ge}$  decays with a half-life of 11.4 days by electron capture to the ground state of  $^{71}\text{Ga}$ . The low-energy mono-energetic Auger electrons and stopped X-rays are detected

in a proportional gas counter.

In the Gallex experiment 30 tons of Gallium (containing 12 tons of  $^{71}\text{Ga}$ ) is dissolved in a very acidic HCl solution. The Gallium is present in the form of  $\text{GaCl}_3$  and the Germanium as  $\text{GeCl}_4$ . It can be separated by bubbling an inert gas (He) through the solution. The efficiency of the Gallex experiment has been tested by applying a very intense ( $6.2 \times 10^{16}$  Bq)  $^{51}\text{Cr}$  sources [9], which was installed for a period of 3.5 months in the Gallex experiment. The exposure to the radioactive  $^{51}\text{Cr}$  source yielded  $1.04 \pm 0.12$  for the ratio of measured over expected  $^{71}\text{Ge}$  events, indicating that the Gallex detection efficiency for low-energy neutrinos is well understood.

In april 1998, the Gallex experiment was succeeded by the GNO experiment [11] in the Gran Sasso mine. At present, GNO and SAGE are the only experiments that can detect neutrinos with a threshold as low as 233 keV. Although SAGE and Gallex/GNO use more than half the world supplies of gallium, the detected neutrino rates in each detector amount to a few per month.

**Kamiokande** is the only first-generation neutrino detection experiment that uses Cerenkov light to detect the neutrinos. It is located 1000 m underground in the Mozumi mine of the Kamioka Mining and Smelting Co. in Kamioka, Japan. In the experiment the Cerenkov light produced by relativistic particles in a tank containing 3000 tons of pure water was collected by about 1000 photomultiplier tubes. Cerenkov radiation occurs when the velocity of the particle  $v$  is larger than the phase velocity of light in the medium that is traversed:

$$v > \frac{c}{n}$$

with  $c$  the speed of light and  $n$  the index of refraction. The light is emitted in a cone around the trajectory of the particle with a maximal angle of  $\cos \theta_{max} = \frac{v}{cn}$ . Each relativistic charged particle will deposit Cerenkov light in a number of scintillators. By analyzing the position and arrival times of the light in the scintillators the vertex, direction, and speed of the particle can be determined. The vertex is very important, since the origin of traversing muons will be at the edge of the water detector. Since there are many times more muons than neutrino events, the most important selection criterion on the data is that the vertex is not close to the edge of the tank.

The Cerenkov technique, applied by Kamiokande, has as disadvantage that the detector is insensitive to neutrinos below 5 - 10 MeV. However, there are also large advantages:

- the **energy** and **direction** of the neutrino can be determined from the distribution of the light in the photomultipliers. A day-night effect or an energy dependence of the neutrino spectrum is observable (relevant for neutrino oscillations in cosmic neutrinos).
- The time of the event can be determined with high accuracy. Indeed, an upper limit to the neutrino mass can be obtained from the 11 neutrino events that were detected at Kamiokande during the supernova explosion SN1987A in 1987.
- The detector is also sensitive to event types: other neutrino species (albeit from much higher energy), cosmic radiation, or proton decay. One of the goals of the Kamiokande detector has been to determine the life time of the proton (set a lower limit or observe proton decay).
- There is no shortage of pure water to build larger detectors.

The detected fluxes of these experiments are given in the table below.

It is clear that the observed neutrino flux is not consistent with the predictions of the standard solar model. Also modifications of the relative importance of each reaction chain is ruled out, due to the different sensitivities of the four experiments. The

Table 4: Neutrino fluxes in SNU for the five discussed experiments[10, 11, 13, 7, ?]. The last column gives the ratio of these fluxes to the standard solar model as discussed in the text.

| Experiment       | Flux (SNU)               | ratio [%]              |
|------------------|--------------------------|------------------------|
| Homestake        | $2.56 \pm 0.16 \pm 0.16$ | $27 \pm 2.5 \pm 4$     |
| Gallex           | $78 \pm 6 \pm 5$         | $61 \pm 5 \pm 7$       |
| GNO              | $66 \pm 10 \pm 4$        | $52 \pm 9 \pm 7$       |
| SAGE             | $68 \pm 7 \pm 4$         | $53 \pm 6 \pm 7$       |
| Super Kamiokande | $2.32 \pm 0.03 \pm 0.08$ | $46 \pm 0.01 \pm 0.04$ |

Kamiokande experiment is only sensitive to the rare  $^8\text{B}$  neutrinos. The observed energy and angular spectrum from solar neutrinos is in agreement with the expected  $^8\text{B}$  spectrum (within statistics). The Chlorine experiment is sensitive to  $^7\text{Be}$  and (mainly)  $^8\text{B}$  neutrinos. The reactions  $^7\text{Be}(e^-, \nu_e)^7\text{Li}$  and  $^7\text{Be}(p, \gamma)^8\text{B}$  compete. Models, in which there are less  $^8\text{B}$  neutrinos and more  $^7\text{Be}$  neutrinos cannot explain the rates of the Chlorine and Kamiokande experiment simultaneously. Furthermore it has been suggested that the p-p chain is less important and the C-N-O chain more important. However, then the observed fluxes should be much higher. It can be concluded that either at least three of the four experiments (both Gallium and either Kamiokande or Homestake) is in error, or the standard model must be changed. There are no solar models on the market that can explain the rate discrepancy. It may be possible that physics beyond the standard electroweak model change the energy spectrum or flavor content of the neutrinos in between the center of the sun and the detector in the earth. The most plausible candidate for such an effect is the mechanism of neutrino oscillations, discussed in the next section.

## 1.4 Neutrino oscillations

In the standard model, neutrinos only couple to W and Z bosons in the weak interaction if they are left-handed (and anti-neutrinos right-handed). The mass of the neutrinos is small, but not necessarily zero. Furthermore it is assumed, that lepton family number is conserved, i.e. an electron-neutrino will not convert to a muon-neutrino or a tau-neutrino. This conservation law is not necessarily fulfilled. Note, that the quark families **do** mix (e.g. not only transitions from down to up quarks are mediated by the charged weak current, but also transitions from strange to up quarks). In analogy, it could be possible that also neutrino families do mix, provided that they differ in mass (and that individual lepton family number is not conserved). Such a mixing can explain the deficit of neutrinos observed in the solar neutrino experiments.

The neutrino states  $|\nu_e\rangle$ ,  $|\nu_\mu\rangle$ , and  $|\nu_\tau\rangle$  that are produced in the weak interaction are called **flavor** or **current eigenstates**. The flavor eigenstates are linear combinations of the **mass eigenstates**, the states that diagonalize the free Hamiltonian. The mass eigenstates describe the free neutrino wave function. The wave function of an electron neutrino can be expanded in the wave function of the mass eigenstates.

The flavor eigenstates  $\nu_e$ ,  $\nu_\mu$ ,  $\nu_\tau$  will be denoted with greek subscripts ( $\nu_\alpha, \nu_\beta, \dots$ ). They can be represented by linear combinations of the mass eigenstates, denoted by numerical subscripts ( $\nu_1, \nu_2, \dots$ ). The development in time of a state  $|\nu_\alpha\rangle$ , that was initially a flavor eigenstate, can be written as

$$|\nu_\alpha \rangle_t = \sum_j U_{\alpha j} e^{-iE_j t} |\nu_j \rangle \quad (2)$$

with  $U_{\alpha j}$  a unitary matrix that can be chosen real in the case of CP-conservation. In analogy,  $U$  in the quark sector is given by the Cabibbo-Kobayashi-Maskawa mixing matrix (which is complex, since the CP symmetry is violated in the  $K_0$ -system). For simplicity in the representation, the states  $|\nu_j \rangle$  are assumed to be eigenstates of the momentum; hence each state  $|\nu_j \rangle$  has a slightly different energy  $E_j = \sqrt{p^2 + m_j^2}$ , with  $m_j$  the (small) neutrino mass. The amplitude for observing an initially created neutrino state  $|\nu_\alpha \rangle$  after some time as a state  $|\nu_\beta \rangle$  is given by

$$\langle \nu_\beta | \nu_\alpha \rangle_t = \sum_j U_{\alpha j} U_{\beta j}^* e^{-iE_j t}. \quad (3)$$

The probability for a transition from the state  $|\nu_\alpha \rangle$  to the state  $|\nu_\beta \rangle$  is given by

$$|\langle \nu_\beta | \nu_\alpha \rangle_t|^2 = \sum_{j,k} U_{\alpha j} U_{\beta j}^* U_{\alpha k}^* U_{\beta k} e^{-i(E_j - E_k)t}. \quad (4)$$

For typical solar neutrino applications, the average over neutrino energies causes the oscillating terms to cancel out for  $j \neq k$  (see [14]). Ignoring oscillatory terms, the smallest possible neutrino flux is found by minimizing the probability for an electron neutrino to remain an electron neutrino, subject to the condition that the total probability for all transitions is unity (that is the reason to require a unitary matrix  $U$ . One does not want to have neutrinos disappearing spontaneously, or be created from the vacuum spontaneously). This condition is obtained when all the matrix products  $|U_{ei}|^2$  are equal, resulting in a probability of  $1/N$  for  $N$  flavors (i.e.  $1/3$ ). In this case, the electron neutrino has an equal overlap with all three mass eigenstates. This is sufficient to explain the results of the Kamiokande and Homestake experiments, but only barely. In the quark sector, the mixing between families is substantially less than maximal. However, efficient reduction of the amount of solar electron-neutrinos can be obtained by matter-enhanced mixing, the so-called MSW-effect, which was proposed by Wolfenstein [15, 16] and Mikheyev and Smirnov [17], as will be discussed later.

First, we will consider vacuum oscillations. The mechanism of neutrino oscillations can be understood by considering only 2 flavors, which is done here for simplicity. The flavor eigenstates  $|f \rangle$  can be expressed in the mass eigenstates  $|m \rangle$  with the aid of a two-dimensional orthogonal matrix which can be chosen real without loss of generality:

$$|f \rangle = U_{vac} |m \rangle, \quad U_{vac} = \begin{pmatrix} \cos \theta_{vac} & \sin \theta_{vac} \\ -\sin \theta_{vac} & \cos \theta_{vac} \end{pmatrix}. \quad (5)$$

Here,  $\theta_{vac}$  denotes the mixing angle in vacuum. Without loss of generality, we can choose  $0 \leq \theta_{vac} \leq \frac{\pi}{4}$ , so that  $|\nu_e \rangle$  is mostly  $|\nu_1 \rangle$ . The second flavor eigenstate  $|\nu_\beta \rangle$  may be identified with muon neutrinos, tau neutrinos, a linear combination of them, or with a hypothetical fourth-generation neutrino. The time evolution of an electron-neutrino in vacuum is then written as

$$|\nu_e \rangle_t = \cos \theta_{vac} e^{-iE_1 t} |\nu_1 \rangle + \sin \theta_{vac} e^{-iE_2 t} |\nu_2 \rangle,$$

with the probability of an electron-neutrino to keep the same flavor as

$$|\langle \nu_e | \nu_e \rangle_t|^2 = 1 - \sin^2 2\theta_v \sin^2\left(\frac{E_2 - E_1}{2}t\right). \quad (6)$$

The energy difference for relativistic neutrinos at the same momentum is

$$E_2 - E_1 = \frac{m_2^2 - m_1^2}{2E} \equiv \frac{\pm \Delta m^2}{2E}$$

(the plus sign applies if  $m_2 > m_1$ , the minus sign in the opposite case). The magnitude of vacuum mixing is proportional to  $\sin^2 \theta_{vac}$ , which may be expected to be small, since the analogous term in quark mixing between the down quark and the strange quark, described by the Cabibbo angle, is  $\sin^2 \theta_{Cabibbo} = 0.05$ . If  $\theta_{vac}$  has the same magnitude, then the average expected probability for an electron-neutrino to survive is about 90 %. The vacuum oscillation length, defined as

$$L_{vac} \equiv \frac{4\pi E}{\Delta m^2} = 2.48 \left(\frac{E}{\text{MeV}}\right) \left(\frac{\text{eV}^2}{\Delta m^2}\right) \text{m},$$

is often used in oscillation experiments performed with reactor beams or accelerators. For solar neutrinos, it is convenient to express  $L_{vac}$  in terms of astronomical units. The time-dependent dimensionless argument of the sine function in Eq. 6 is then expressed as

$$\frac{\pi R}{L_{vac}} = 1.9 \times 10^{11} \frac{1 \text{ MeV}}{E} \frac{\Delta m^2}{1 \text{ eV}^2} \frac{R}{1 \text{ AU}}.$$

Solar neutrino experiments are sensitive to mass differences where the argument  $\frac{\pi R}{L_{vac}}$  can significantly affect the probability of observing an electron neutrino at earth.

#### 1.4.1 Matter Oscillations

The arbitrary neutrino state in the previous section can be rewritten in terms of a Schrödinger equation, with a mass matrix representing the Hamiltonian. It is written as

$$|\nu \rangle_t = c_e(t)|\nu_e \rangle + c_x(t)|\nu_x \rangle.$$

The matrix describing the time dependence of an arbitrary state expressed in the flavor basis can be obtained by differentiating  $|\nu_e \rangle$  and  $|\nu_x \rangle$  with respect to time. One obtains

$$M_{vac,flavor} = \begin{pmatrix} a_1 & b \\ b & a_2 \end{pmatrix} \quad (7)$$

with

$$a_1 = \frac{m_1^2 \cos^2 \theta_{vac} + m_2^2 \sin^2 \theta_{vac}}{2E},$$

$$a_2 = \frac{m_1^2 \sin^2 \theta_{vac} + m_2^2 \cos^2 \theta_{vac}}{2E},$$

and

$$b = \frac{\Delta m^2 \sin 2\theta_{vac}}{4E}.$$

In the presence of matter, the mass matrix  $M$  becomes  $M = M_{vac} + M_{matter}$ . A description of  $M_{matter}$  was first given by Wolfenstein [15, 16], who pointed out that neutrino-electron scattering contributes a term to the mass matrix that is not present in vacuum. The charged current, which is present in  $(\nu_e, e^-)$  scattering, but not for the other neutrino flavors (see Fig. 8) is the origin of this matter term. Wolfenstein found, that  $M_{matter}$  can be written as

$$M_{matter} = \sqrt{2}G_F n_e |\nu_e \rangle \langle \nu_e|,$$

with  $n_e$  the electron density. For anti-electron-neutrinos, the term has the same magnitude, but the opposite sign. The time development of the wave function in matter can be written in analogy to the vacuum wave function as

$$i \frac{d}{dt} \begin{pmatrix} c_e(t) \\ c_x(t) \end{pmatrix} = \begin{pmatrix} a_1 + \sqrt{2}G_F n_e & b \\ b & a_2 \end{pmatrix} \begin{pmatrix} c_e(t) \\ c_x(t) \end{pmatrix}, \quad (8)$$

If  $\theta_{vac}$  is small, the mixing of the neutrino states is small in vacuum. However, one obtains complete mixing if in the presence of matter the resonance condition  $a_1 + \sqrt{2}G_F n_e = a_2$  occurs. One obtains

$$i \frac{d}{dt} (c_e - c_x) = (a - b)(c_e - c_x)$$

with  $a = a_1 + \sqrt{2}G_F n_e = a_2$ . This condition is fulfilled for

$$n_e = \frac{(m_2^2 - m_1^2) \cos 2\theta_{vac}}{2\sqrt{2}EG_F}.$$

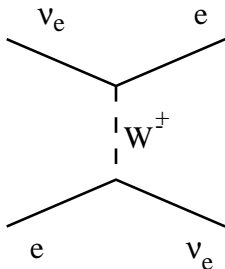


Figure 5: Feynman diagram contributing to electron- $\nu_e$  scattering, but not to neutrinos of other flavors.

This can happen if  $m_1 < m_2$  (if the electron neutrino has the largest overlap with the heavier neutrino mass eigenstate, then a resonance will occur for **anti-electron-neutrinos** in the presence of electrons). This could happen in the sun for small vacuum mixing angles ( $\approx 10^{-3}$ ) and  $m_2^2 - m_1^2$  as small as a few times  $10^{-5} \text{ eV}^2$ . Since the neutrino, originating at the center of the sun, encounters a steadily decreasing electron density, the MSW-effect can in principle even completely remove electron neutrinos, if the adiabatic condition is fulfilled that the electron density varies sufficiently slowly (see Fig. 1.4.1).

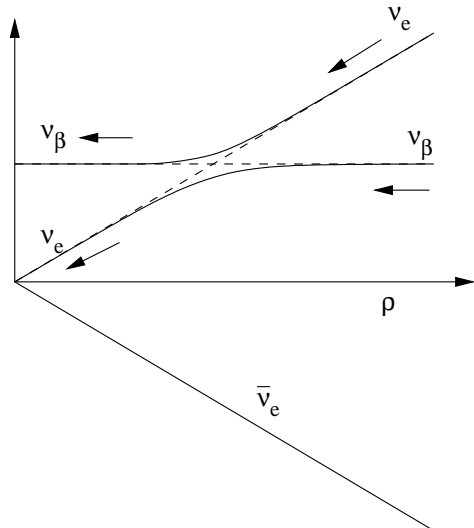


Figure 6: Transformation of electron neutrinos, created at high electron densities, to neutrinos with flavor  $\beta$  at low densities, for the case that the electron density  $\rho$  changes adiabatically. Alternatively, a neutrino with flavor eigenstate  $\beta$  may be transformed in an electron-neutrino when it is directed towards the high density region (the center of the sun).

## 1.5 Second generation neutrino detectors

The solar neutrino problem, and the successful operation of the first generation of neutrino detectors, has inspired many experimental groups to develop second generation cosmic neutrino detectors. These constitute multi-purpose experiments: not only do the various groups try to obtain more data on solar neutrinos, but also cosmic neutrinos are studied (matter oscillations through the earth, high-energetic cosmic neutrinos, ratio of muon and electron neutrinos as well as anti-neutrinos) and other processes like proton decay. Some of these detectors are described here.

Super-Kamiokande [18] is the follow-up of the Kamiokande experiment. It commenced data-taking in 1996. As active medium it also uses water, but the detector is about 10 times larger in size. It contains 50,000 cubic meters of pure water, divided in an outer tank and an inner tank. The outer tank is used to shield the detector from charged particles originating from cosmic radiation or radioactive decay in the surrounding earth material. The inner tank is monitored by 11,146 20-inch photomultiplier tubes. They are arranged in such a way, that the vertex of the event can be determined. In this way, contributions from charged particles originating outside the detector are further reduced.

Super-Kamiokande reported already more solar neutrino events than all four first-generation experiments together in 1999. The first result [19] has been published in *Phys. Rev. Lett.*. They found in a 504 day period from June 1996 to March 1998 a result of  $0.474^{+0.010}_{-0.009} \quad ^{+0.017}_{-0.014}$ , with the first range of errors the experimental uncertainty, and the second range of errors the uncertainty on the solar standard model as claimed by Bahcall [5]. The experimental energy spectrum is also in good agreement with the calculated solar  ${}^8\text{B}$ -spectrum [19]. In 2001, Bahcall updated their model, using new data on the low-energy ( ${}^7\text{Be}(p, {}^8\text{B})$ ) reaction. In 2002, Super kamiokande published their result for 1464 days of data taking [?]. The latest value for the ratio equals  $0.460 \pm 0.06 \pm 0.10$ ,

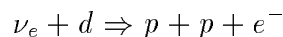
where the large theoretical uncertainty is due to the calculation of the  ${}^8B$  neutrino flux.

For solar neutrinos, no day-night effect has been observed. This implies, that the amount of neutrinos observed is not modified by passing through an earth- radius of material. This may be not surprising, since solar neutrinos already passed through the sun, which contains much more material. Apart from solar neutrinos, also atmospheric neutrinos are measured. Super-Kamiokande claims to have evidence for neutrino oscillations [20]. One expects the ratio of 2  $\mu$  neutrinos for 1 electron-neutrino from atmospheric neutrinos. (Cosmic radiation is mainly due to high-energetic protons. In the outer atmosphere these protons undergo collisions producing lots of pions, which decay into (anti-)muons and (anti-)muon-neutrinos.(Depending on the muon-energy,) the vast majority of these muons decay before they reach the Super-Kamiokande detector, leaving an electron (or positron), an (anti-)electron neutrino and an (anti-)muon neutrino. Therefore, one expects 2 muon neutrinos per atmospheric electron neutrino. The observed ratio in Super-Kamiokande is however less than 2. Moreover, the ratio differs for events coming from “above” which traversed relatively little material, and from “below”, where up to 12,000 km of earth has been traversed. This difference in the ratio of electron to muon neutrinos can be explained by assuming  $\nu_\mu - \nu_\tau$  oscillations. The mixing angle for these oscillations is then large, and the mass difference between  $m_3^2$  and  $m_2^2$  should be in the order of  $10^{-4}$  eV<sup>2</sup>.)

Apart from solar and atmospheric neutrino research, the Kamiokande detector is also used to test the standard model by determining limits for the proton life time (no proton decay has been observed yet), and magnetic monopole flux. Furthermore, high-energetic cosmic radiation is studied.

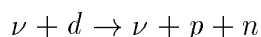
Super Kamiokande was the first second-generation experiment that published results. Here we will describe some other second-generation neutrino experiments. The Sudbury Neutrino Observatory (SNO) [21] studies neutrinos from the sun and cosmological sources. It will measure the flux and energy spectrum of electron neutrinos, as well as the total flux of all neutrino types above 2.2 MeV. It is located 2073 meters below the ground in a mine in northern Ontario (Canada). The detector uses heavy water (D<sub>2</sub>O) instead of water; therefore it is capable of distinguishing between electron-neutrinos and other flavor neutrinos, by looking at the events in which deuterium breaks up. Three reactions play an important role:

- Charged current.



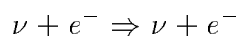
This reaction is sensitive to electron neutrinos. The Cerenkov light of the emitted electron will be detected.

- neutral current.



The charged current cross section is the same for every neutrino and anti-neutrino flavor. The gamma rays emitted when the thermalized neutron is captured by a nucleus will liberate electrons (from other atoms), of which the Cerenkov light is detected.

- Electron scattering.



This process is not specific for SNO. It is sensitive to all neutrino species, but the cross section for electron neutrinos is about 6 times higher than for the other neutrino species. The expected rate is about 10 % of the charged-current event rate.

The SNO-experiment is made possible due to the fact that the Canadian government has been stockpiling deuterium, which was produced in nuclear reactors. The SNO experiment uses 900 m<sup>3</sup> D<sub>2</sub>O and 1700 m<sup>3</sup> H<sub>2</sub>O in the central detector, and 5300 m<sup>3</sup> of H<sub>2</sub>O around the central detector. The water has been purified, it contains less than 10<sup>-14</sup> g/g of Uranium and Thorium isotopes. Cerenkov light is detected with 10,000 photomultipliers.

The SNO experiment recently published first results, both for the elastic scattering reaction, the charged current reaction, and the neutral current reaction [22]. For the charged-current reaction they measured a neutrino flux of  $(1.76 \pm 0.06 \pm 0.09) \times 10^6 \nu/cm^2/s$ , whereas the standard solar model [?] predicted  $5.05 \times 1.00^{+0.20}_{-0.16}$ . This result, together with the higher SuperKamiokande elastic scattering rate of  $2.32 \pm 0.03 \pm 0.08$ , gave the first experimental evidence that solar neutrinos mix. SNO also published results for elastic scattering (where also mu and tau neutrinos contribute, although with lower cross section) and for the neutral current interaction. For elastic scattering, they deduced a flux of  $2.39 \pm 0.24 \pm 0.12$ , in agreement with the higher-statistics result of SuperKamiokande. For the neutral current interaction, they deduced a total solar neutrino flux of  $5.09 \pm 0.44^{+0.46}_{-0.43}$ , in excellent agreement with the prediction of Bahcall. Therefore, the SNO experiment gave strong evidence for neutrino oscillations.

The Borexino collaboration [24] applies a well-shielded, ultrapure liquid scintillator detector with a mass of 300,000 kg. It is located in the Gran Sasso mine in Italy. The liquid is monitored by 2200 photomultipliers. As in the other experiments, the detector is shielded by a layer of water to reduce background from charged particles coming from outside. It is specialized in detecting low-energy neutrinos with high resolution. The threshold is 250 keV, well below the mono-energetic <sup>7</sup>Be line, but above the pp-neutrinos. Its high resolution and low energy threshold makes it very suitable for solar neutrino physics. A second liquid scintillator is operated in Japan by the KamLand experiment [25]. This experiment aims for measuring the disappearance of electron anti-neutrinos by measuring the flux of these neutrinos, generated by commercial nuclear power plants in Japan. They submitted a paper to Physics Review Letters, indicating a 4 -  $\sigma$  observation of disappearance of these nnti-neutrinos.

Other detectors use arctic ice (AMANDA [26]) or deep-sea water (e.g. Antares [27] in the mediterranean) as a medium to obtain a truly gigantic detector. (E.g. Antares aims for a cubic kilometer of water (10<sup>12</sup> kg) as the active medium). These detectors are well suited to study high energetic cosmic events.

## 1.6 Neutrino parameters.

In this subsection, an overview of the current knowledge on neutrino parameters is given. For the most recent updates see the particle data group (on the web at <http://pdg.web.cern.ch/pdg/>) and the continuously refreshed neutrino page of Juha Peltoniemi (<http://cupp.oulu.fi/neutrino/>).

### Families of neutrinos.

From the LEP data on the width of the Z<sub>0</sub> boson, we know that the number of light lepton families is  $2.984 \pm 0.008$ . A hypothetical light fourth-generation neutrino that

couples weakly to the  $Z_0$  boson is hence ruled out.

### Neutrinoless double beta decay.

Neutrinos do not carry chargelike quantities as far as known. Therefore, they may be their own anti-particle. A particle that is its own anti-particle is called a Majorana particle. In the standard model, the neutrino carries lepton number, and it is not equal to its own anti-particle (Dirac neutrinos). In many extensions of the standard model however, the neutrino is a Majorana particle. If the neutrino is a Majorana particle, neutrinoless double-beta decay could occur (the lepton number is violated by 2 units), see Fig. 1.6. Also in models with non-leptonnumber conserving right-handed currents, neutrinoless double beta decay may occur. The relevant phenomenological part of the hamiltonian is given by

$$H_W = \frac{G_F}{2} \times \{J_L j_L^\dagger + \kappa J_R j_L^\dagger + \eta J_L j_R^\dagger + \lambda J_R j_R^\dagger\} + h.c. \quad (9)$$

where  $j_L = \bar{e}_L \gamma^\mu \nu_{eL}$  is the normal left-handed lepton current,  $j_R = \bar{e}_R \gamma^\mu \nu_{eR}$ , and  $J_L$  and  $J_R$  are the left-handed and right-handed hadronic weak currents.

Searches for neutrinoless double beta decays in nuclear systems have been conducted for decades. The nuclear double-beta decay experiments are not sensitive to  $\kappa$  in the equation above (here, the *nuclear* current is righthanded), but limits are placed on the standard-model violating terms  $\lambda$  and  $\eta$ . For massless neutrinos, or neutrinos without mixing, the quantities  $\eta$  and  $\lambda$  disappear. The limits that can be placed from these measurements depend on the calculation of the nuclear matrix elements in the transitions, for which the spread in different concurrent models are up to a factor of 5 (depending on the parent nucleus). Calculated half-lives of typical nuclear targets used in these experiments ( $^{76}\text{Ge}$ ,  $^{82}\text{Se}$ ,  $^{100}\text{Mo}$ ,  $^{136}\text{Xe}$ ) are around  $10^{24} - 10^{25}$  years. Again, these experiments are very challenging in terms of background suppression and single-event detection. Limits on  $\eta$  are in the order of  $10^{-8}$ , limits on  $\lambda$  are in the order of  $10^{-6}$ . The Moscow-Heidelberg group presented a positive  $3\sigma$  result for neutrinoless double-beta decay [23].

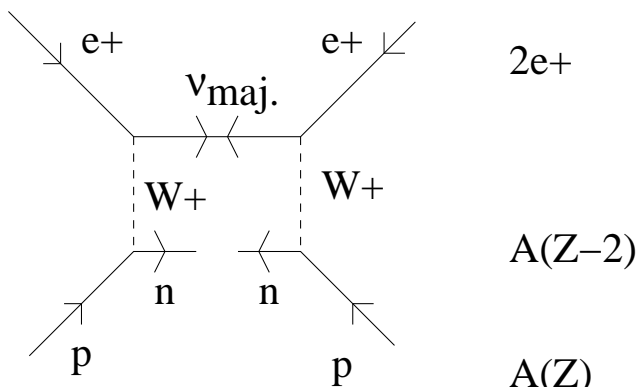


Figure 7: Neutrinoless double beta decay  ${}^Z A \rightarrow {}^{Z-2} A e^+ e^+$ , in which two protons are converted to two neutrons, and two positrons are created. The connecting line between the two positrons is the majorana neutrino, which is its own anti-particle (the mass term in the Lagrangian for Majorana neutrinos makes this diagram possible).

### Solar neutrinos.

As seen in the section on solar neutrinos, the disappearance of electron neutrinos from the sun can be explained by vacuum oscillations only when all three flavors mix almost maximally and  $\Delta m^2 = 8 \times 10^{-11} \text{ eV}^2$ . However, it can be explained in terms of matter oscillations via the MSW mechanism when the mixing angle is small (order  $\sin^2 2\theta \simeq 6 \times 10^{-3}$ ) and the mass difference between the electron neutrino and the neutrino-flavor into which it oscillates is around  $10^{-5} \text{ eV}^2$ .

### Atmospheric neutrinos.

In Super-Kamiokande an excess of electron neutrinos with respect to muon neutrinos is observed. Simultaneously, the ratio for multi-GeV muon-neutrinos coming from above ( $\cos \theta > 0.2$ ) or below ( $\cos \theta < -0.2$ ) through the earth is  $0.52 \pm 0.05$ , indicating that muon-neutrinos disappear. All atmospheric neutrino data from Super-kamiokande can be described when one assumes, that muon neutrinos oscillate into tau-neutrinos, with  $2 \times 10^{-3} \text{ eV}^2 < \Delta M^2 < 6 \times 10^{-3} \text{ eV}^2$  and maximal mixing,  $\sin^2 2\theta \simeq 1$ .

### LSND

Neutrino oscillations are also studied with neutrino factories. Again one can study the disappearance, by having detectors at different distances in the neutrino beam, or appearance, by looking at the appearance of other-flavor neutrinos in the beam. Only one experiment, LSND, has seen a positive signal. The LSND experiment studied neutrinos from a beam created by stopped positively-charged pions, which decay via the chain  $\pi^+ \rightarrow \mu^+ \nu_\mu; \mu^+ \rightarrow e^+ \nu_e \bar{\nu}_\mu u$ . An excess of anti-electron neutrinos  $\bar{\nu}_e$ , which are not produced in this chain, has been reported [28]. Since for this experiment  $\frac{L}{E} \sim 1 \text{ km/GeV}$ , the implied mass splitting is  $\Delta M^2 > 1 \text{ eV}^2$ . LSND finds supporting evidence for this oscillation in an independent study, using the decay of pions in flight at different energies [29]. However, other experiments do not observe these fluctuations, and rule out part of the LSND parameter space.

### A minimal scheme.

Lets see how one could bring into agreement the results from solar neutrinos, atmospheric neutrinos, and LSND via oscillation. We have seen, that the mass differences in these mechanisms are of three different orders of magnitude. This cannot be brought into agreement with the existence of only 3 flavors of neutrinos, since we have then only 2 independent mass differences  $\Delta M^2$ . We therefore introduce a hypothetical fourth flavor, which has to be a sterile neutrino (i.e. it does not couple to the normal weak interaction gauge bosons), else it would influence the  $Z_0$  decay width.

Such a 4-flavor scheme can account for all observed neutrino oscillation measurements. We need a nearly degenerate pair  $\nu_2, \nu_3$  with masses close to 1 eV, and a much lighter pair  $\nu_1, \nu_0$ , with the mass of the  $\nu_0$  around  $3 \times 10^{-3}$  and  $M_1 \ll M_0$ . The mass splitting  $M_2$  and  $M_3$  is assumed to be around  $4 \times 10^{-3} \text{ eV}^2$ , to be compatible with the atmospheric neutrino data. Then the muon and tau neutrinos are about 50-50 % mixtures of  $\nu_2$  and  $\nu_3$ . The splitting  $M_0^2 - M_1^2 \sim 10^{-5} \text{ eV}^2$  allows for a description of the solar neutrino problem in terms of the MSW effect. The electron neutrino, which is mainly the lighter

$\nu_1$  is then converted to the unobserved sterile neutrino  $\nu_0$ . The mass splitting of about 1 eV between the light and the heavy pair may then describe the LSND results. Of course, other scenarios are possible, and particularly the LSND result needs to be verified.

## References

- [1] J. N. Bahcall, M. H. Pinsonneault, and G. J. Wasserburg, *Rev. Mod. Phys.* **67**, 781 (1995).
- [2] J. N. Bahcall and R. K. Ulrich, *Rev. Mod. Phys.* **60**, 297 (1988).
- [3] J. N. Bahcall *et al.*, *Physics Today* 30 (July 1996).
- [4] R. B. Leighton, R. W. Noyes, and G. W. Simon, *Astrophys. J.* **135**, 474 (1962).
- [5] J. N. Bahcall, Sarbani Basu, and M. H. Pinsonneault, *Phys. Lett. B* **433**, 1 (1998).
- [6] T. Toutain and C. Fröhlich, *Astron. Astrophys.* **257**, 287 (1992).
- [7] B. T. Cleveland *et al.*, *Nucl. Phys. B* **38** (proc. suppl.), 47 (1995); *Astrophys. J.* **496**, 505 (1998).
- [8] P. Anselmann *et al.*, *Phys. Lett. B* **285**, 376 (1992).
- [9] P. Anselmann *et al.*, *Phys. Lett. B* **342**, 440 (1995).
- [10] W. Hampel *et al.* *Phys. Lett. B* **447**, 127 (1999).
- [11] N. Ferrari, *Nucl. Phys. B. Proc. Suppl.* **91**, 44 (2001). Workshop, Conca Specchiulla (Otranto), Spet. 2000,
- [12] M. Altmann *et al.*, *Phys. Lett. B* **490**, 16 (2000).
- [13] J. N. Abdurashitov *et al.*, *Phys. Lett. B* **328**, 234 (1994); *Phys. Rev. C* **60**, 0055801 (1999).
- [14] J. N. Bahcall and S. C. Frautschi, *Phys. Lett. B* **29**, 263 (1969).
- [15] L. Wolfenstein, *Phys. Rev. D* **17**, 2369 (1978).
- [16] L. Wolfenstein, *Phys. Rev. D* **20**, 2634 (1979).
- [17] S.P. Mikheyev and A. Yu. Smirnov; *Sov. J. Nucl. Phys* **42**, 193 (1986); *Sov. Phys. - JETP* **64**, 4 (1986); *Nuovo Cimento C* **9**, 17 (1986).
- [18] <http://www-sk.icrr.u-tokyo.ac.jp/doc/sk/index1.html>
- [19] *Measurement of the Solar Neutrino Energy Spectrum Using Neutrino-Electron Scattering*, the Super-Kamiokande collaboration, *Phys. Rev. Lett.* **81**, 1562 (1998); Y. Fukuda *et al.*, *Phys. Rev. Lett.* **87**, 071301 (2001).
- [20] the Super-Kamiokande collaboration, *Phys. Rev. Lett.* **81**, 1562 (1998); and *Phys. Rev. Lett.* **85**, 3999 (2000).
- [21] <http://www.sno.phy.queensu.ca>
- [22] Q.R. Ahmad *et al.*, *Phys. Rev. Lett.* **89**, 0011302 (2002).
- [23] H.V. Klapdor-Kleingrothaus *et al.*, *Mod. Phys. Lett.* **16**, 2409 (2001).

- [24] <http://almime.mi.infn.it>
- [25] <http://www.awa.tohoku.ac.jp/html/KamLand/index.html>
- [26] <http://amanda.berkeley.edu>
- [27] <http://antares.in2p4.fr/antares>
- [28] C. Athanassopoulos *et al.*, *Phys. Rev.* **C54**, 2685 (1996); and *Phys. Rev. Lett.* **77**, 3082 (1996).
- [29] C. Athanassopoulos *et al.*, *Phys. Rev. Lett* **81**, 1774 (1998); and *Phys. Rev.* **C58**, 2511 (1998).